Flexible operation of modular electrochemical CO_2 reduction processes

K. Roh * **L. C. Brée** ** **P. Schäfer** ** **D. Strohmeier** ** **A. Mitsos** **

* *Department of Chemical Engineering and Applied Chemistry, Chungnam National University, 34141 Daejeon, Republic of Korea (e-mail: ksroh@cnu.ac.kr).*
** *Process Systems Engineering (AVT.SVT), RWTH Aachen University, 52074 Aachen, Germany*

Abstract: Electrochemical CO_2 reduction (eCO_2R) is an emerging technology that is capable of producing various organic chemicals from CO_2, but its high electricity cost is a big economic obstacle. One solution to reduce the cumulative electricity cost is demand side management, i.e., to adjust the power load based on time-variant electricity prices. However, varying the power load of CO_2-electrolyzers often leads to changes in Faraday efficiency towards target components and thereby influences the product composition. Such deviations from the target product composition may be undesired for downstream processes. We tackle this challenge by proposing a flexible operating scheme for a modular eCO_2R process. We formulate the economically optimal operation of an eCO_2R process with multiple electrolyzer stacks as a parallel-machine scheduling problem. Adjusting the power load of each sub-process properly, we can save electricity costs while the desired product composition is met at any time. We apply an algorithm based on wavelet transform to solve the resulting large-scale nonlinear scheduling problem in tractable time. We solve each optimization problem with a deterministic global optimization software MAiNGO. We examine flexible operation of a modular eCO_2R process for syngas production. The case studies show that the modular structure enables savings in the cumulative electricity cost of the eCO_2R process via flexible operation while deviations in the syngas composition could be reduced. Also, the maximum ramping speed of the entire process is found to be a key parameter that strongly influences the cost saving.

Keywords: Electrochemical CO_2 reduction; Demand side management; Modularization; Parallel-machine scheduling; Nonlinear scheduling; Wavelet transform

1. INTRODUCTION

Electrochemical carbon dioxide (CO_2) reduction (eCO_2R) is an emerging technology that is capable of producing various organic chemical compounds out of CO_2. Being integrated with renewable energy systems, eCO_2R has been known as a promising alternative to conventional fossil-based chemical production. Recent research on eCO_2R has focused on synthesis of novel catalysts for the production of, e.g., carbon monoxide, formic acid, ethylene, and ethanol (De Luna et al., 2019). In addition, electrode and reactor design (Vennekoetter et al., 2019), conceptual process design (Chae et al., 2020), and techno-economic and sustainability analysis (Roh et al., 2020) are of interest as well.

The electricity cost is one of the major cost drivers of eCO_2R technologies (Jouny et al., 2018). A straightforward solution to the electricity cost reduction is to lower the overpotential of, particularly, the anode oxygen evolution reaction (Sun et al., 2017). On the other hand, if an eCO_2R process is powered by grid electricity, one can adjust the plant load to fluctuations in electricity (spot) prices. This flexible operation, namely demand side management (DSM) or demand response (DR), leads to savings in overall electricity costs (Daryanian et al., 1989). In academia, DSM has been applied to various industrial plants, such as air separation units, chlor-alkali plants, and aluminium plants (Mitsos et al., 2018).

A major challenge of flexible operation of eCO_2R processes is that the composition of the effluent stream depends on the current density (or applied voltage). For example, increasing the current density of CO_2-electrolyzers dedicated to syngas (a mixture of hydrogen and carbon monoxide) production leads to a higher H_2/CO ratio due to the changes in the Faraday efficiencies toward hydrogen and carbon monoxide (Vennekötter et al., 2019). The deviation of the product composition from the nominal level is typically undesired for downstream processes. This feature is distinct from other conventional electrolysis, such as water electrolysis and chlor-alkali electrolysis, in which the product concentrations do not significantly change with respect to the current density. To meet the product specification, a part of the components should be separated, which would complicate the process configuration and worsen the economic viability as well.

To tackle this challenge, we propose a flexible operation of modular eCO_2R processes. Motivated from the parallel

machine scheduling (Jans, 2009), an eCO_2R process consists of N identical sub-processes that can be operated independently from one another. Adjusting the power load of each sub-process properly according to the instantaneous electricity prices rather than keeping the power load fixed, we can save the overall electricity costs while the desired product concentration can be met.

We formulate scheduling problems to determine the optimal load profile of each sub-process. In this study, syngas is chosen as a target product of an eCO_2R process. Since the syngas production rate and power requirement are represented as nonlinear functions of the current density, we solve nonlinear scheduling problems. In order to reduce the computational cost, we apply our recently proposed algorithm based on wavelet transform (Schäfer et al., 2020). We conduct a sensitivity analysis that perturbs the maximum ramping speed of each sub-process to see how much it influences the electricity cost savings.

2. SYSTEM DESCRIPTION

Figure 1 depicts the block flow diagram of an eCO_2R process, which is modularized and thus capable of running flexibly. The entire system consists of N identical sub-processes that are independently operable. Herein, we consider a moderate size of N ($2 \sim 8$). Carbon dioxide and water are fed into electrolyzer stacks in each sub-process and then target chemicals are synthesized at the cathode chambers via electrochemical CO_2 reduction reactions. Meanwhile, oxygen, a byproduct, is generated in the anode chambers.

Recent studies on electrochemical CO_2 reduction have reported per-pass conversion of CO_2 below 35% (Jouny et al., 2018). Thus, the significant amount of unreacted CO_2 remains in the cathode effluent streams and has to be separated by a CO_2 separation unit(s). In this study, we introduce N identical CO_2 separation units connected to N CO_2-electrolyzer stacks to treat the respective cathode effluent. The separated CO_2 is then preferably recycled for reducing the CO_2 feed cost.

To enable DSM, the process requires overcapacity, meaning that we install more than the minimum number of electrolyzer cells needed to achieve the target production rate. In addition, the products from all the stacks are mixed and stored in a storage tank. This intermediate storage is mandatory for the constant supply of the product to the downstream process.

3. MATHEMATICAL FORMULATION

The scheduling model presented below is developed to determine the optimal operation of each sub-process of an eCO_2R process. The following assumptions are made:

- quasi-steady-state model with discrete-time variables;
- perfect forecast of electricity prices in the day-ahead market;
- no side-product generated;
- unreacted CO_2 in the cathode effluent is completely removed;
- considering power demand for electrolysis only.

3.1 Mass balances

The molar amount of a component c produced by stack s at time step t ($n_{s,c,t}$) is calculated by

$$n_{s,c,t} = \frac{\mathrm{FE}_{s,c,t}\, j_{s,t}\, A_{\mathrm{Cell}}\, N_{\mathrm{Cell}}}{F\, z_c}\, \Delta t, \quad \forall s \in S, c \in C, t \in T, \quad (1)$$

where $\mathrm{FE}_{s,c,t}$ denotes the Faraday efficiency toward component c of stack s, $j_{s,t}$ the current density of stack s, A_{Cell} the active electrode area, N_{Cell} the number of cells per stack, Δt the length of time step, F the Faraday constant, and z_c the number of electrons transferred. Note that $\mathrm{FE}_{s,c,t}$ of CO_2-electrolyzers often sharply varies with respect to $j_{s,t}$. For example, when a silver catalyst is applied to the cathode, the CO_2 reduction reaction that generates CO is superior at low current density due to its low onset potential while the hydrogen evolution reaction becomes dominant at high current density (Vennekoetter et al., 2019). Therefore, this dependency should be properly represented by exploiting either experiment or simulation data.

The total amount of each component and the target product is calculated by

$$n_{c,t} = \sum_s n_{s,c,t}, \quad \forall c \in C, t \in T, \quad (2)$$

$$n_{\mathrm{Prod},t} = \sum_c n_{c,t}, \quad \forall t \in T. \quad (3)$$

To maintain the product quality, an additional constraint is imposed:

$$Q(n_{c,t}) = q_{\mathrm{Prod}}, \quad \forall t \in T. \quad (4)$$

where $Q(n_{c,t})$ calculates the product quality as a function of $n_{c,t}$, e.g., the H_2/CO molar ratio of syngas, and q_{Prod} is the target value.

We consider the amount of the stored product limited to the maximum storage capacity C_{Prod}:

$$-\frac{C_{\mathrm{Prod}}\, n^N_{\mathrm{Prod}}}{2\,\Delta t} \leqslant \sum_{\tau=1}^{t} (n_{\mathrm{Prod},\tau} - n^N_{\mathrm{Prod}}) \leqslant \frac{C_{\mathrm{Prod}}\, n^N_{\mathrm{Prod}}}{2\,\Delta t}, \quad \forall t \in T, \quad (5)$$

where n^N_{Prod} is the nominal production level. Initially, half of the storage tank is assumed to be filled by the product.

3.2 Power consumption

The power consumption at time step t can be calculated by

$$P_t = \sum_s (j_{s,t}\, A_{\mathrm{cell}}\, U_{s,t}\, N_{\mathrm{Cell}})\, \Delta t, \quad \forall t \in T, \quad (6)$$

where $U_{s,t}$ denotes the cell potential of stack s at time step t. As the current density $j_{s,t}$ increases, the cell potential $U_{s,t}$ rises due to, for example, the activation and ohmic overpotentials.

3.3 Ramping constraints

Suitable ramping constraints should be imposed in order to make the quasi-steady state assumptions adequate for optimizing the operation of the dynamic systems, such as

$$-\Delta j \leqslant j_{s,t} - j_{s,t-1} \leqslant \Delta j, \quad \forall s \in S, t \in T, \quad (7)$$

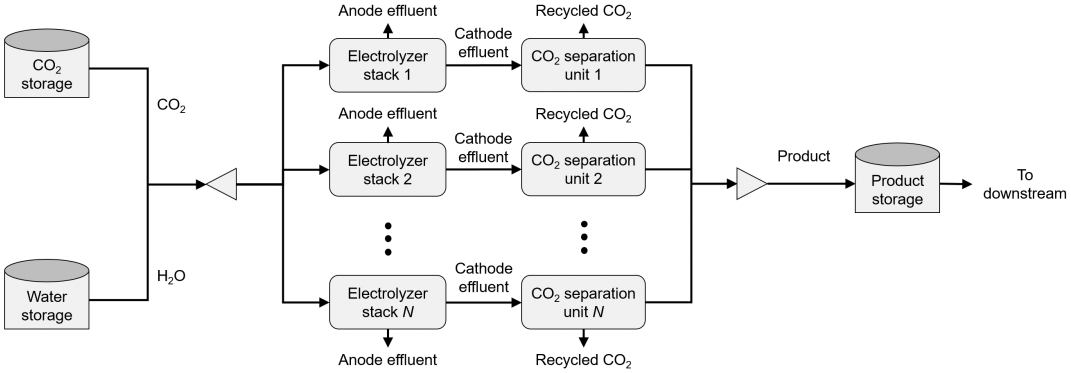

Figure 1. Block flow diagram of a generalized modular eCO_2R process for chemical production

where Δj denotes the maximal ramping speed. Δj is calculated by

$$\Delta j = \frac{j^{max} - j^{min}}{T_{\text{Ramp}}}, \tag{8}$$

where j^{max} and j^{min} denote the maximal and minimal allowable current density, respectively. T_{Ramp} denotes the minimal ramping duration between the two extreme operating points.

3.4 Symmetry-breaking constraints

We impose the lexicographic ordering constraints (Sherali and Smith, 2001) that exclude alternative solutions to break the symmetry and shorten the computation time accordingly:

$$j_{s,t} \geqslant j_{s+1,t}, \quad \forall s = \{1...S_T - 1\}, t \in T, \tag{9}$$

where S_T is the total number of stacks. This constraint forces, for example, the current density of Stack 1 to be higher than those of other stacks over the simulation horizon.

3.5 Objective function

We minimize the sum of the electricity costs over the time horizon:

$$\min_{j_{s,t}} \sum_t p_t P_t, \tag{10}$$

where p_t denotes an electricity spot price.

4. CASE STUDY

We demonstrate the proposed operation concept on a syngas production system based on co-electrolysis of CO_2 and H_2O. Four identical and independently operable sub-processes produce syngas via the following electrochemical reactions over Ag catalysts:

$$2\,H^+ + 2\,e^- \longrightarrow H_2$$
$$CO_2 + 2\,H^+ + 2\,e^- \longrightarrow CO + H_2O.$$

We choose a desired H_2/CO molar ratio of 1, which is suitable for liquid fuel synthesis via the Fisher-Tropsch process with iron-based catalysts (de Smit and Weckhuysen, 2008) and oxo-synthesis for isomeric aldehydes production (Billig and Bryant, 2005). Therefore,

$$n_{\text{H}_2,t}/n_{\text{CO},t} = q_{\text{Syn}}, \quad \forall t \in T, \tag{11}$$

where $q_{\text{Syn}} = 1$ and $n_{\text{H}_2,t}$ and $n_{\text{CO},t}$ are the total molar amount of H_2 and CO produced at time step t. Each sub-process comprises one CO_2-electrolyzer stack and one CO_2 separation unit. Each stack consists of 30 electrolyzer cells, so the total number of electrolyzer cells is 120. The total syngas production rate is 5.87 kmol/h, which can be manufactured by 100 electrolyzer cells operated at the nominal current density (117 mA/cm^2) determined by Brée et al. (2020). The effective area of one electrolyzer cell is assumed to be 2.7 m^2, which is the size of the typical chlor-alkali electrolyzer cell (O'Brien et al., 2005). The syngas storage is capable of supplying syngas to a downstream for maximum of six hours (C_{Syn}). The time step size is an hour.

The design of the electrochemical reactor (f) in Vennekötter et al. (2019) is adapted to the electrolyzers considered in this case study. It is a proton exchange membrane (PEM) reactor with zero-gap configuration at the anode and a silver gas diffusion electrode (GDE) at the cathode. Brée et al. (2020) developed a dynamic model, which was validated to the experimental data of the aforementioned reactor setup. Using the developed model, we generate the Faraday efficiency and cell potential at different current density as plotted in Figure 2-(a) and (c).

The original dynamic model for calculation of Faraday efficiency and cell potential are highly nonlinear, so they are not suitable to the scheduling model. We derive the cubic polynomial functions $f^{\text{FE}}_{s,c,t}$ and $f^{\text{U-j}}_{s,t}$ as the surrogate functions of $\text{FE}_{s,c,t}\, j_{s,t}$ (*effective* current density) in (1) and $U_{s,t}\, j_{s,t}$ (power density) in (6) as follows:

$$f^{\text{FE}}_{s,c,t} = \text{FE}_{s,c,t}\, j_{s,t} = \alpha_{\text{FE},c}\, j^3_{s,t} + \beta_{\text{FE},c}\, j^2_{s,t} + \gamma_{\text{FE},c}\, j_{s,t} + \delta_{\text{FE},c}, \quad \forall s \in S, c \in \{\text{H}_2, \text{CO}\}, t \in T, \tag{12}$$

$$f^{\text{U-j}}_{s,t} = U_{s,t}\, j_{s,t} = \alpha_P\, j^2_{s,t} + \beta_P\, j_{s,t} + \gamma_P, \quad \forall s \in S, t \in T, \tag{13}$$

where α, β, γ, and δ are the coefficients of the surrogate functions. The underlying and surrogate functions are plotted in Figure 2-(b) and -(d). Note that, in Vennekötter

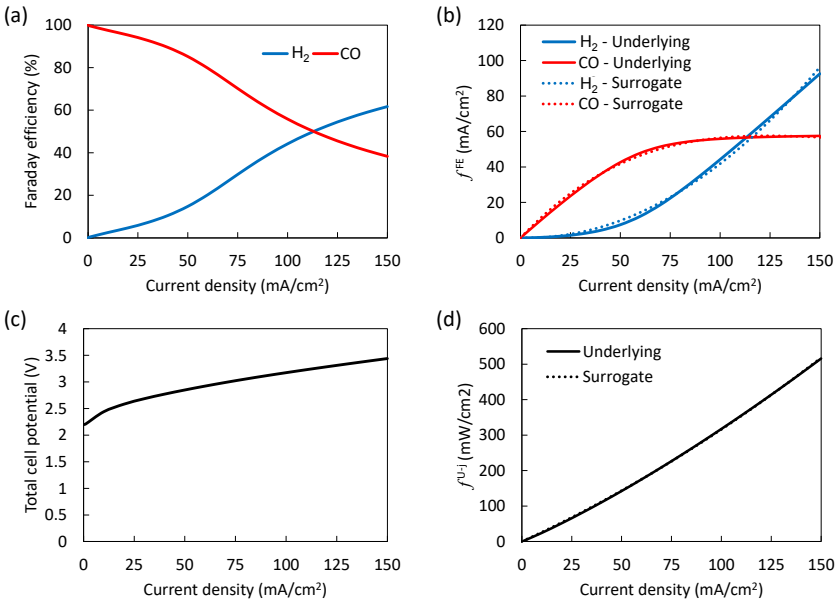

Figure 2. Faraday efficiency (a) and cell potential (c) of the CO_2-electrolyzer; and the underlying and surrogate functions of f^{FE} (b) and $f^{\mathrm{U\text{-}j}}$ (d). The simulation results and underlying functions are taken from Brée et al. (2020). The errors of the surrogate functions are below 1%.

et al. (2019), the current density is measured up to 100 mA/cm^2. In this study, we extrapolate the Faraday efficiency and cell potential at the current density of 100 to 150 mA/cm^2 with the rigours dynamic model of Brée et al. (2020).

Regarding the removal of bulk CO_2 from syngas, several technical candidates are available, such as chemical absorption, adsorption and membrane gas separation. These options differ in energy demand, operating and capital expenses, and dynamic responses. In this study, we assume that the unreacted CO_2 is separated via an arbitrary separation technology. As mentioned in Section 3, we exclude the energy demand for CO_2 separation because it is much smaller than the energy demand for electrolysis. For example, CO_2 is assumed to be separated by pressure swing adsorption (PSA) that demands approximately 1.75 $\mathrm{GJ_{elec}/t_{CO_2}}$ (Bui et al., 2018). This amounts to only 11.5% of the power demand of co$_2$-electrolysis at the nominal current density (assuming 30 % of CO_2 per-pass conversion). Note that the energy demand of PSA given in Bui et al. (2018) is required for capturing CO_2 from flue gases, of which the CO_2 concentration is below 20 mol.%. As the CO_2 concentration of the cathode effluent of the CO_2-electrolyzer stack would be much higher (up to 50 mol.%), the specific energy demand for the CO_2 separation would be even lower (see Hasan et al. 2014).

Dynamic responses of electrochemical reactions are generally fast, e.g., water electrolysis (Buttler and Spliethoff, 2018), so the CO_2 separation unit is likely to limit the ramping speed of the sub-processes (T_{Ramp}). Possible technologies for CO_2 separation would differ in the ramping speed. For instance, membrane gas separation and PSA allow fast ramping (DiMartino et al., 1988; Sinha and Padhiyar, 2019) while chemical absorption (Jung et al., 2020) takes longer time to change the operation level. In order to investigate how much the maximal ramping speed affects the optimal operation as well as the cost savings, we assume different values of T_{Ramp} (one to three hours).

An hourly electricity spot price profile (Figure 3) for three days is taken from the German EPEX SPOT market, recorded end of May in 2018 (Agora Energiewende, 2019).

Our optimization problem is a nonlinear program due to the nonlinear surrogate functions $f^{\mathrm{FE}}_{s,c,t}$ and $f^{\mathrm{U\text{-}j}}_{s,t}$. Nonlinear scheduling problems are rarely solved because they are computationally challenging to obtain global solutions. To tackle this challenge, linear approximation is usually applied to reformulate the problem into mixed-integer linear programs, e.g., Zhang et al. (2016), however, such an approximation could generate inaccurate results. Instead, we apply the wavelet-based grid adaptation algorithm (Schäfer et al., 2020). We can find near-optimal solutions of (nonlinear) scheduling problems in a tractable time by using a few optimization variables only. Moreover, this algorithm always creates feasible schedule as the correct nonlinear models can be used. Herein, the current density $j_{s,t}$ are the optimization variables. The entire horizon (144 h) comprises two time intervals (128 and 16 steps) concatenated. As a result, the number of degrees of freedom is greatly reduced compared to 574 (144 × 4) in the original problem. The mathematical models are implemented in our in-house open-source software for deterministic global optimization MAiNGO (Bongartz et al., 2018) based on McCormik relaxation (McCormick, 1976; Mitsos et al., 2009).

The simulation results are illustrated in Figure 3. The results show that the optimal current density of each stack is adjusted to the time-variable electricity prices

while at anytime meeting the H_2/CO ratio of the mixed syngas stream entering the syngas storage. Because of the symmetry-breaking constraints (9) imposed, Stack 1 and Stack 4 always operate at the highest and lowest current densities, respectively. Interestingly, more than two stacks occasionally follow the same trajectory, e.g., Stack 2 and 3 in the case of 2 hr of the maximal ramping duration. This kind of optimal trajectories would facilitate the process control in practice. During the period of low electricity prices, some stacks are operated at relatively high current density, which results in not only the higher syngas production rate but also the higher H_2/CO ratio than the nominal levels (see Figure 2-(a)). Other stacks, however, run at below the nominal current density due to the syngas ratio constraint (11).

As shown in Figure 3, the shorter the maximal ramping duration, the more dynamical the operation of the sub-processes. As a result, more dynamic operation ends up with higher savings in the cumulative electricity cost compared to the steady operation at the nominal current density. It indicates that employing a CO_2 separation unit that allows fast changes in the operation level will considerably improve the overall economics of the modular eCO_2R system by DSM.

5. CONCLUSION

We proposed the modularization of an electrochemical CO_2 reduction process for the purpose of reducing the electricity costs by demand side management. The modularization is an effective operation strategy to meet a certain product quality while properly shifting the power demand of individual sub-processes. We formulated a nonlinear scheduling problem to minimize the cumulative electricity costs of an electrochemical system while optimizing the operation of each sub-process. The case study demonstrated our operation idea on co-electrolysis of CO_2-H_2O for the production of syngas. The entire system is made of four sub-processes, each of which produces syngas and separates unreacted CO_2 independently. We used the wavelet-based grid adaptation algorithm to obtain near-optimal solutions in a reasonable computation time. The simulation results suggest that the flexible operation of the modular process can reduce the electricity costs while maintaining the syngas ratio. Moreover, the maximum ramping speed of the sub-process, which is likely to be determined by the CO_2 separation unit, is found to be a key factor that has a considerable impact on cost savings.

For future research, we should investigate the influences of other parameters, e.g., the degree of modularization (i.e., the number of sub-processes) and the strength of electricity price fluctuation, on cost savings. Also, additional capital costs required for employing flexible operation and modular configuration should be analyzed. Particularly, installing a fewer number of large CO_2 separation units is worth investigating because of benefits from economies-of-scale.

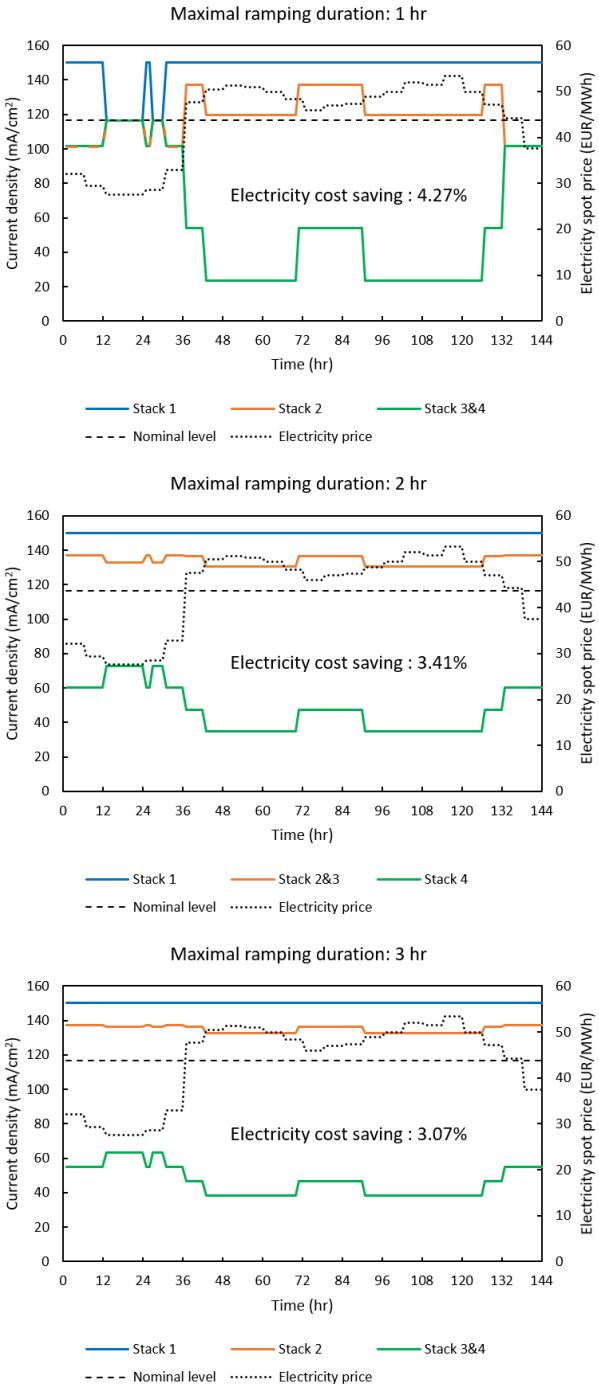

Figure 3. Profiles of the current density of the four stacks in the eCO_2R process and their expected electricity cost savings for different maximal ramping duration. The power load of the reference case ($N = 1$) running at the nominal level is fixed in time.

ACKNOWLEDGEMENTS

The authors gratefully acknowledge the financial support of the Kopernikus-project "SynErgie" by the Federal Ministry of Education and Research (BMBF) and the project supervision by the project management organization Projektträger Jülich (PtJ). This research was funded by Chungnam National University. Financial support from National Research Foundation of Korea (NRF) funded by the Ministry of Education (2020M3H7A109636112) is greatly acknowledged. We are also grateful to Dr. Dominik Bongartz, Marc-Daniel Stumm, and Dennis Grasmik for their support of implementing MAiNGO models.

REFERENCES

Agora Energiewende (2019). https://www.agora-energiewende.de/de/themen/-agothem-/Produkt/produkt/76/Agorameter/. Data accessed: 15-Nov-2019.

Billig, E. and Bryant, D.R. (2005). Oxo Process. In *Van Nostrand's Encyclopedia of Chemistry*. John Wiley & Sons, Inc., Hoboken, NJ, USA. doi:10.1002/0471740039.vec1832.

Bongartz, D., Najman, J., Sass, S., and Mitsos, A. (2018). MAiNGO - McCormick-based Algorithm for mixed-integer Nonlinear Global Optimization. Technical report, RWTH Aachen University, Aachen, Germany.

Brée, L.C., Wessling, M., and Mitsos, A. (2020). Modular modeling of electrochemical reactors: Comparison of CO2-electolyzers. *Computers & Chemical Engineering*, 139, 106890.

Bui, M., Adjiman, C.S., Bardow, A., Anthony, E.J., Boston, A., Brown, S., Fennell, P.S., Fuss, S., Galindo, A., Hackett, L.A., Hallett, J.P., Herzog, H.J., Jackson, G., Kemper, J., Krevor, S., Maitland, G.C., Matuszewski, M., Metcalfe, I.S., Petit, C., Puxty, G., Reimer, J., Reiner, D.M., Rubin, E.S., Scott, S.A., Shah, N., Smit, B., Trusler, J.P.M., Webley, P., Wilcox, J., and Mac Dowell, N. (2018). Carbon capture and storage (CCS): the way forward. *Energy & Environmental Science*, 11(5), 1062–1176.

Buttler, A. and Spliethoff, H. (2018). Current status of water electrolysis for energy storage, grid balancing and sector coupling via power-to-gas and power-to-liquids: A review. *Renewable and Sustainable Energy Reviews*, 82(September 2017), 2440–2454.

Chae, S.Y., Lee, S.Y., Han, S.G., Kim, H., Ko, J., Park, S., Joo, O.S., Kim, D., Kang, Y., Lee, U., Hwang, Y.J., and Min, B.K. (2020). A perspective on practical solar to carbon monoxide production devices with economic evaluation. *Sustainable Energy & Fuels*, 4(1), 199–212.

Daryanian, B., Bohn, R.E., and Tabors, R.D. (1989). Optimal demand-side response to electricity spot prices for storage-type customers. *IEEE Transactions on Power Systems*, 4(3), 897–903.

De Luna, P., Hahn, C., Higgins, D., Jaffer, S.A., Jaramillo, T.F., and Sargent, E.H. (2019). What would it take for renewably powered electrosynthesis to displace petrochemical processes? *Science*, 364(6438), eaav3506.

de Smit, E. and Weckhuysen, B.M. (2008). The renaissance of iron-based Fischer–Tropsch synthesis: on the multifaceted catalyst deactivation behaviour. *Chemical Society Reviews*, 37(12), 2758.

DiMartino, S., Glazer, J., Houston, C., and Schott, M. (1988). Hydrogen/carbon monoxide separation with cellulose acetate membranes. *Gas Separation & Purification*, 2(3), 120–125.

Hasan, M.M.F., Boukouvala, F., First, E.L., and Floudas, C.A. (2014). Nationwide, Regional, and Statewide CO2 Capture, Utilization, and Sequestration Supply Chain Network Optimization. *Industrial & Engineering Chemistry Research*, 53(18), 7489–7506. doi:10.1021/ie402931c.

Jans, R. (2009). Solving Lot-Sizing Problems on Parallel Identical Machines Using Symmetry-Breaking Constraints. *INFORMS Journal on Computing*, 21(1), 123–136.

Jouny, M., Luc, W., and Jiao, F. (2018). General Techno-Economic Analysis of CO2 Electrolysis Systems. *Industrial & Engineering Chemistry Research*, 57(6), 2165–2177.

Jung, H., Im, D., Heo, S., Kim, B., and Lee, J.H. (2020). Dynamic analysis and linear model predictive control for operational flexibility of post-combustion CO2 capture processes. *Computers & Chemical Engineering*, 140, 106968.

McCormick, G.P. (1976). Computability of global solutions to factorable nonconvex programs: Part I — Convex underestimating problems. *Mathematical Programming*, 10(1), 147–175.

Mitsos, A., Asprion, N., Floudas, C.A., Bortz, M., Baldea, M., Bonvin, D., Caspari, A., and Schäfer, P. (2018). Challenges in process optimization for new feedstocks and energy sources. *Computers & Chemical Engineering*, 113(c), 209–221.

Mitsos, A., Chachuat, B., and Barton, P.I. (2009). McCormick-Based Relaxations of Algorithms. *SIAM Journal on Optimization*, 20(2), 573–601.

O'Brien, T.F., Bommaraju, T.V., and Hine, F. (2005). *Handbook of Chlor-Alkali Technology*. Springer US, Boston, MA. doi:10.1007/b113786. URL http://link.springer.com/10.1007/b113786.

Roh, K., Bardow, A., Bongartz, D., Burre, J., Chung, W., Deutz, S., Han, D., Heßelmann, M., Kohlhaas, Y., König, A., Lee, J.S., Meys, R., Völker, S., Wessling, M., Lee, J.H., and Mitsos, A. (2020). Early-stage evaluation of emerging CO2 utilization technologies at low technology readiness levels. *Green Chemistry*, 22(12), 3842–3859.

Schäfer, P., Schweidtmann, A.M., and Mitsos, A. (2020). Nonlinear scheduling with time-variable electricity prices using sensitivity-based truncations of wavelet transforms. *AIChE Journal*, 66(10), 1–12.

Sherali, H.D. and Smith, J.C. (2001). Improving Discrete Model Representations via Symmetry Considerations. *Management Science*, 47(10), 1396–1407.

Sinha, P. and Padhiyar, N. (2019). Optimal startup operation of a pressure swing adsorption. *IFAC-PapersOnLine*, 52(1), 130–135.

Sun, Z., Ma, T., Tao, H., Fan, Q., and Han, B. (2017). Fundamentals and Challenges of Electrochemical CO2 Reduction Using Two-Dimensional Materials. *Chem*, 3(4), 560–587.

Vennekoetter, J.B., Sengpiel, R., and Wessling, M. (2019). Beyond the catalyst: How electrode and reactor design determine the product spectrum during electrochemical CO2 reduction. *Chemical Engineering Journal*, 364(September 2018), 89–101.

Vennekötter, J.B., Scheuermann, T., Sengpiel, R., and Wessling, M. (2019). The electrolyte matters: Stable systems for high rate electrochemical CO2 reduction. *Journal of CO2 Utilization*, 32(April), 202–213.

Zhang, Q., Grossmann, I.E., Sundaramoorthy, A., and Pinto, J.M. (2016). Data-driven construction of Convex Region Surrogate models. *Optimization and Engineering*, 17(2), 289–332.